EPJ manuscript No.
(will be inserted by the editor)

An example of quantum imaging: rendering an object undetectable

Stefan Ataman[1]

Extreme Light Infrastructure - Nuclear Physics (ELI-NP), 30 Reactorului Street, 077125 Magurele, Romania e-mail: stefan.ataman@eli-np.ro

Received: date / Revised version: date

Abstract. In this paper we propose and analyse a Gedankenexperiment involving three non-linear crystals and two objects inserted in the idler beams. We show that, besides the behaviour that can be extrapolated from previous experiments involving two crystals and one object, we are able to predict a new effect: under certain circumstances, one of the objects can be rendered undetectable to any single detection rate on the signal photons with discarded idler photons. This effect could find applications in future developments of quantum imaging techniques.

PACS. PACS-key describing text of that key – PACS-key describing text of that key

arXiv:1604.07617v1 [quant-ph] 26 Apr 2016

1 Introduction

The non-linear optical process of spontaneous parametric down-conversion (SPDC) [1,2,3] creates pairs of highly entangled single photon pairs [4,5]. Its use became ubiquitous in quantum optics (QO), where numerous experiments rely on this process [6,7,8,9,10,11,12,13].

SPDC is a process that happens randomly, somehow in the spirit of spontaneous emission of an excited atom. However, in an experiment by Ou, Wang, Zou and Mandel [9,10], two non-linear crystals fed by the same pump laser show a phenomenon of "phase memory". A landmark experiment using two non-linear crystals was performed by Zou, Wang and Mandel [11]. Its counter-intuitive feature stemmed from the fact that the singles count rate of the two interfering signal beams shows or does not show interference effects in function of the distinguishability/indistinguishability of the discarded idler beams. Based on this principle, the imaging of small objects using undetected (discarded) photons has been recently experimentally demonstrated [12]. One can now use a wavelength where the object is transparent and detect photons of another wavelength, more convenient for the detectors [12]. This idea is pushed even further out of the lab and towards industrial applications by Kalashnikov et al. in reference [14] where they perform infrared spectroscopy yet they use red photons at the detectors. For a review on quantum imaging techniques and implementations one can consult reference [15].

With these latest developments, it becomes obvious that the field of quantum imaging is still in its infancy and many developments are to be expected in the near future.

In this paper, we show that an object can be rendered undetectable using the already proven principle of quantum imaging with discarded idler photons [11,12]. We propose the extension of the experiment from reference [11] to the case involving three non-linear crystals. Besides the expected behaviour (i.e. the extension of the counter-intuitive features of the results of Zou et al. [11]), we show that, under certain circumstances, the second object can be rendered invisible to any photo-counters if the idler photons are discarded.

This paper is organized as follows. In Section 2 the proposed experiment is introduced and qualitatively discussed. Its complete quantum optical description is thoroughly developed in Section 3. The computation of various single and coincidence photo-detection rates is done in Section 4. Finally, conclusions are drawn in Section 5.

2 The proposed experiment

In the proposed Gedankenexperiment three non-linear crystals are pumped together by a common laser (see Fig. 1). We assume that the pumping power of each individual crystal can be adjusted at will. The crystals are aligned in such a way, that the idler mode of NL_1 (i_1) is overlapping the idler modes of NL_2 (i_2) and NL_3 (i_3). Therefore, a photo-detection at detector D_I would not be able to tell from which nonlinear crystal the photon originated. The signal modes of NL_1 (s_1) and NL_2 (s_2) are brought together into the beam splitter BS_a. Its first output leads to the photo-detector D_A, while the second one enters the beam splitter BS_b, where it combines with the signal mode of NL_3 (s_3). The two outputs of this beam splitter lead to

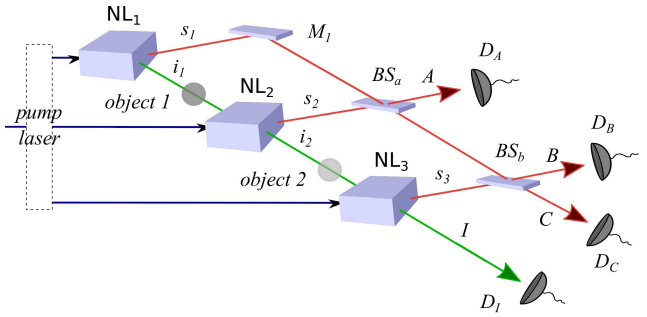

Fig. 1. The proposed experiment. Three non-linear crystals are pumped by a common laser. The idler modes of the crystals overlap, therefore become indistinguishable. The signal modes are brought to interfere through the beam splitters BS_a and BS_b. The two objects can be inserted in the gray regions of i_1 and i_2.

the photo-detectors D_B and D_C. Throughout this paper, we assume ideal and broad-band photo-detectors.

More or less transparent objects can be inserted in the dashed regions of the beams i_1 and i_2 (see Fig. 1).

If we do not pump the non-linear crystal NL_3 and consider single rates at the detector D_A, we find ourselves in the experimental setup described by Zou, Wang and Mandel [11]. Therefore, the same counter-intuitive behavior is expected, with the singles detection rate at D_A depending on the transmissivity of the inserted object (called "object 1") into the beam i_1.

At a first glance, the extension to three crystals and two objects seems trivial and devoid of surprises. Inserting an object (called thereafter "object 2") into the beam i_2 should be detected by a variation of the singles rate at either D_B or D_C.

In the following, we will show that this is not always the case. For some well chosen parameters of object 1, beam splitter BS_a and the pumping powers of NL_1 and NL_2, object 2 can simply become invisible (regardless of its transmissivity) to any single detection rate at D_A, D_B or D_C. Therefore, if we discard the idler photons, there is no way to detect object 2. Even coincidence counts $D_B - D_I$ and $D_C - D_I$ fail to reveal its presence.

3 The quantum optical description of the experiment

In the SPDC process, the input beam (generally called "pump", p) is split into two output beams (generally called "signal" s and "idler" i). This process takes place at the single photon level: one input photon is destroyed and two output photons are created. Energy ($\hbar\omega$) and momentum ($\hbar\boldsymbol{k}$) conservation requirements (also called "phase matching conditions") impose frequency ($\omega_p = \omega_s + \omega_i$) and wavenumber ($\boldsymbol{k}_p \approx \boldsymbol{k}_s + \boldsymbol{k}_i$) relations between the input-output fields.

We shall make a number of simplifying assumptions. Similar to references [11,12,13,20] we shall consider all modes as being monochromatic. Since the phase relation between the three pump fields can be fixed at any value, we simply assume that all crystals are pumped in phase, yielding

$$|\psi_{\mathrm{in}}\rangle = \frac{1}{\mathcal{N}}\left(\gamma_1|1_{p_1}\rangle + \gamma_2|1_{p_2}\rangle + \gamma_3|1_{p_3}\rangle\right) = \frac{\left(\gamma_1\hat{a}^\dagger_{p_1} + \gamma_2\hat{a}^\dagger_{p_2} + \gamma_3\hat{a}^\dagger_{p_3}\right)}{\mathcal{N}}|0\rangle \qquad (1)$$

where $\mathcal{N}$ is a normalization constant, $|1_{p_k}\rangle$ denotes a Fock state with one photon in mode (port) p_k, $\hat{a}^\dagger_{p_k}$ denotes the usual input creation operator in mode p_k with $k = 1, 2, 3$ and $|0\rangle$ is the vacuum state. A detailed discussion of this choice is given in Appendix A. The γ_k parameters with $k = 1, 2, 3$ (assumed real and positive throughout this paper) are connected to input power differences for identical non-linear crystals [21,22]. The quantum state (1) also implies that no two down-conversions happen at the same moment. This is consistent with the low down-conversion efficiency [9,11,13] of the non-linear crystals.

From the perspective of QO, the field operator transformation in each SPDC process is

$$\hat{a}^\dagger_{p_n} \rightarrow \hat{a}^\dagger_{s_n}\hat{a}^\dagger_{i_n} \qquad (2)$$

where $\hat{a}^\dagger_{s_n}$ ($\hat{a}^\dagger_{i_n}$) denotes the signal (idler) creation operators and $n = 1, 2, 3$. The process of SPDC creates pairs of photons from a pump photon in a spontaneous, hence unpredictable way. However, in our model (1) a fixed phase relationship is assumed among the parametric down-conversions (and set to zero for convenience).

With the two objects inserted, the experiment is depicted in Fig. 2. Each object is modelled through a beam splitter [16] having transmission (reflection) coefficients T_m (R_m) and a phase shift φ_m with $m = 1, 2$. Typical BS unitarity constrains [17] apply to these coefficients. The inputs u_m are always in the vacuum mode while the fictitious modes v_m have to be considered, for reasons of unitary evolution of the system (although in the final computation they will be traced out). For a perfectly transparent (opaque) object m we have $T_m = 1$ ($T_m = 0$) with $m = 1, 2$.

For simplicity, in the main part of the paper, the optical lengths of s_1 and s_2 leading to BS_a are assumed to be equal. The same assumption is taken for s_2 and s_3. The scenario with unequal lengths in the signal beams is discussed in Appendix B.

Beam splitters BS_a and BS_b are characterized by the transmission (reflection) coefficients T_n (R_n) with $n = \{a, b\}$. Unitarity requirements impose the well-known conditions $|T_n|^2 + |R_n|^2 = 1$ and $T_n R_n^* + T_n^* R_n = 0$ [17]. Whenever we shall assume balanced beam splitters, we shall replace $T_n = 1/\sqrt{2}$ and $R_n = i/\sqrt{2}$.

After a series of calculations (see details for a slightly more general case in Appendix B), the output state vector

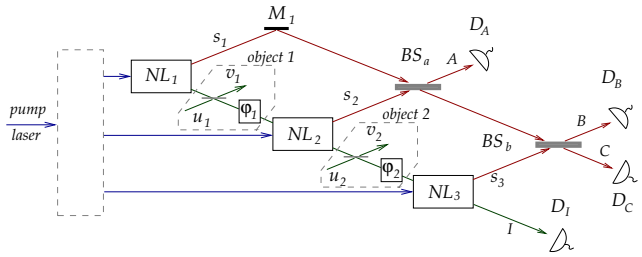

Fig. 2. The objects inserted in the idler beams of NL_1 and, respectively, NL_2 can be modelled by two beam splitters having transmissivity (reflectivity) coefficient T_k (R_k) and two phase delays φ_k with $k = 1, 2$.

is found to be

$$\begin{aligned}|\psi_{\text{out}}\rangle = \frac{1}{\mathcal{N}}\Big(& T_2 \mathrm{e}^{i\varphi_2}\left(\gamma_1 R_a T_1 \mathrm{e}^{i\varphi_1} + \gamma_2 T_a\right)|1_A 1_I\rangle \\ & + R_2\left(\gamma_1 R_a T_1 \mathrm{e}^{i\varphi_1} + \gamma_2 T_a\right)|1_A 1_{v_2}\rangle \\ & + \gamma_1 R_a R_1 |1_A 1_{v_1}\rangle \\ & + \left(R_b T_2 \mathrm{e}^{i\varphi_2}\left(\gamma_1 T_a T_1 \mathrm{e}^{i\varphi_1} + \gamma_2 R_a\right) + \gamma_3 T_b\right)|1_B 1_I\rangle \\ & + R_b R_2\left(\gamma_1 T_a T_1 \mathrm{e}^{i\varphi_1} + \gamma_2 R_a\right)|1_B 1_{v_2}\rangle \\ & + \gamma_1 T_a R_b R_1 |1_B 1_{v_1}\rangle \\ & + \left(T_b T_2 \mathrm{e}^{i\varphi_2}\left(\gamma_1 T_a T_1 \mathrm{e}^{i\varphi_1} + \gamma_2 R_a\right) + \gamma_3 R_b\right)|1_C 1_I\rangle \\ & + T_b R_2\left(\gamma_1 T_a T_1 \mathrm{e}^{i\varphi_1} + \gamma_2 R_a\right)|1_C 1_{v_2}\rangle \\ & + \gamma_1 T_a T_b R_1 |1_C 1_{v_1}\rangle\Big) \end{aligned} \quad (3)$$

where $|1_A 1_I\rangle$ denotes a Fock state with one photon in mode (port) A and one in mode I etc. We construct the density matrix $\hat{\rho}_{\text{out}} = |\psi_{\text{out}}\rangle\langle\psi_{\text{out}}|$ and trace it out over the fictitious modes v_1 and v_2, yielding the reduced density matrix

$$\hat{\rho}_{\text{red}} = \text{Tr}_{v_1,v_2}\left\{\hat{\rho}_{\text{out}}\right\} = \sum_{m,\,n}\langle m_{v_1} n_{v_2}|\hat{\rho}_{\text{out}}|m_{v_1} n_{v_2}\rangle \quad (4)$$

4 Singles and coincidence rates evaluation

Having the reduced density matrix (4) allows one to make all predictions regarding the probabilities of singles or coincidence detections. For example, the singles detection probability at the photo-detector D_A is given by

$$P_A = \text{Tr}\left\{\hat{a}_A^\dagger \hat{a}_A \hat{\rho}_{\text{red}}\right\} \quad (5)$$

and after a short computation one arrives at

$$P_A \sim \left|\gamma_1 R_a T_1 \mathrm{e}^{i\varphi_1} + \gamma_2 T_a\right|^2 + \gamma_1^2 |R_a R_1|^2 \quad (6)$$

It is noteworthy to mention that the dependence on T_2 (R_2) disappears during this computation, therefore the final result from equation (6), as expected, does not depend on the properties of object 2. If one assumes equal pumping powers to NL_1 and NL_2 (i.e. $\gamma_1 = \gamma_2$) and a balanced beam splitter BS_a, equation (6) simplifies to

$$P_A \sim 1 - T_1 \sin(\varphi_1) \quad (7)$$

where we assumed T_1 to be real. This result is similar to the ones already reported [11,12]. Its paradoxical nature arises from the fact that the two idler modes (i_1 and i_2) do not participate in the interference of the signal modes (s_1 and s_2). However, their indistinguishability/distinguishability allows one to have or not to have a quantum state that can be factorized. It is worthwhile to note that the distinguishability/indistinguishability of the beams i_2 and i_3 at the detector D_I plays no role in measuring the probability of detection at P_A.

The singles detection probability at D_B is given by $P_B = \text{Tr}\left\{\hat{a}_B^\dagger \hat{a}_B \hat{\rho}_{\text{red}}\right\}$ and one obtains

$$\begin{aligned} P_B \sim & \left|R_b T_2 \mathrm{e}^{i\varphi_2}\left(\gamma_1 T_a T_1 \mathrm{e}^{i\varphi_1} + \gamma_2 R_a\right) + \gamma_3 T_b\right|^2 \\ & + \left|R_b R_2\left(\gamma_1 T_a T_1 \mathrm{e}^{i\varphi_1} + \gamma_2 R_a\right)\right|^2 + \gamma_1^2 |T_a R_b R_1|^2 \end{aligned} \quad (8)$$

At first sight, this result is simply the extension of equation (6) to the case involving three crystals and two objects. However, one can select values of γ_1, γ_2, T_a, T_1 and φ_1 so that

$$\gamma_1 T_a T_1 \mathrm{e}^{i\varphi_1} + \gamma_2 R_a = 0 \quad (9)$$

In this case, equation (8) simplifies to

$$P_B \sim \gamma_1^2 |T_a R_b R_1|^2 + \gamma_3^2 |T_b|^2 \quad (10)$$

In other words, the presence or absence of object 2 has no influence on the singles photo-count result at D_B. A similar result is obtained at the detector D_C, namely

$$P_C \sim \gamma_1^2 |T_a T_b R_1|^2 + \gamma_3^2 |R_b|^2. \quad (11)$$

Even more counter-intuitive is the coincidence count result at detectors D_B and D_I, yielding

$$P_{B-I} \sim \gamma_3^2 |T_b|^2 \quad (12)$$

or, similarly, at detectors D_C and D_I, giving

$$P_{C-I} \sim \gamma_3^2 |R_b|^2 \quad (13)$$

The question arises: did object 2 become completely undetectable if we obey the condition from equation (9)? The answer is "almost". With the current configuration, we could probe the presence of object 2 by measuring the single counts at D_I or the coincidence counts at D_A and D_I. The latter, for example, yields

$$P_{A-I} \sim \gamma_1^2 |T_1 T_2|^2 / |R_a|^2 \quad (14)$$

a result depending, indeed, on T_2. However, if we discard the idler photons (as done in reference [12]), object 2 is completely invisible to any single detection rates.

5 Conclusions

In this paper we proposed and discussed an experiment able to render undetectable – using quantum, rather than classical principles – a more or less transparent object. For well chosen experimental parameters (including only the first object), a condition for the undetectability of the second object can be obtained. In this case, no matter what properties the second object has, its presence or absence will remain undetected to all single detection rates if the idler photons are discarded.

Acknowledgments

The author wishes to thank Dr. Radu Ionicioiu for useful suggestions for the final form of the manuscript and Dr. Waleed Mouhali for helping him double-check the main results of this paper. The author also wishes to thank the anonymous reviewers for their help in improving this paper.

A About the input state of the system

Equation (1) might seem to be awkward, since the inputs of the non-linear crystals are actually intense coherent fields, while we consider them as being single-photon Fock states. In order to justify this choice, we first write the input state as a coherent state $|\alpha_{p_n}\rangle$ with $n = 1, 2, 3$ and expanding it in Fock state yields

$$|\alpha_{p_n}\rangle = e^{-|\alpha_{p_n}|^2/2}\left(|0\rangle + \alpha_{p_n}\hat{a}^\dagger_{p_n}|0\rangle + \frac{\left(\alpha_{p_n}\hat{a}^\dagger_{p_n}\right)^2}{2}|0\rangle + \dots\right) \tag{15}$$

The only term from equation (15) that yields two photons after the the down-conversion process (2) is the second one. This down-conversion process has a (typically low) efficiency g_n where this coefficient is connected to the $\chi^{(2)}$ nonlinearity of each crystal. Therefore, if we denote $\gamma_n = |\alpha_n| g_n$ and assume post-selection of the two-photon state only (higher order nonlinear processes are negligible) takes us to the input state given by equation (1). If one wants to avoid any higher-order nonlinear process in the crystals, number-resolving photo-detectors (e. g. superconducting nanowire [23]) can be used instead of the usual ones.

A similar result for the output state vector can be obtained by considering the signal and idler modes initially in the vacuum mode and by applying a parametric interaction Hamiltonian [11,15].

B Computing the field operator transformations

Contrary to Section 3, we assume the lengths of the signal beams to the beam splitters non-equal. Therefore, for example, the path length difference (delay) in the beams

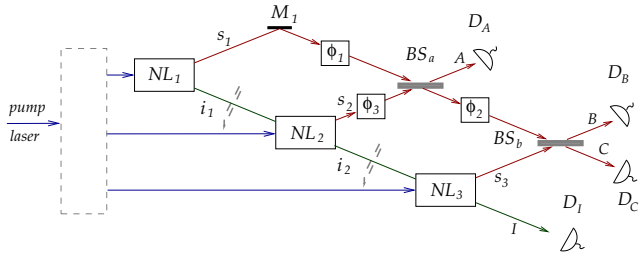

Fig. 3. The experiment in the general case. Path length differences are modelled through phase delays ϕ_1, ϕ_2 and ϕ_3, as depicted above.

s_1 and s_2 is modelled by the phase shift ϕ_1. Additional delays can be added, as depicted in Fig. 3.

The singles/coincidence detection rates we are interested in can be obtained in several ways. One could follow the approach from reference [13] or the one from reference [20]. Here, we sketch another way of computing them, using a graphical method introduced in [18] and extended to non-linear optics in [19]. We can draw the graph associated to our experiment as depicted in Fig. 4 and one obtains the field operator transformations

$$\hat{a}^\dagger_{p_1} = \gamma_1\left(R_a e^{i\phi_1}\hat{a}^\dagger_A + T_a R_b e^{i(\phi_1+\phi_2)}\hat{a}^\dagger_B + T_a T_b e^{i(\phi_1+\phi_2)}\hat{a}^\dagger_C\right) \times\left(T_1 e^{i\varphi_1}T_2 e^{i\varphi_2}\hat{a}^\dagger_I + T_1 e^{i\varphi_1}\hat{a}^\dagger_{v_2} + R_1\hat{a}^\dagger_{v_1}\right) \tag{16}$$

$$\hat{a}^\dagger_{p_2} = \gamma_2\left(T_a e^{i\phi_3}\hat{a}^\dagger_A + R_a R_b e^{i(\phi_2+\phi_3)}\hat{a}^\dagger_B + R_a T_b e^{i(\phi_2+\phi_3)}\hat{a}^\dagger_C\right) \times\left(T_2 e^{i\varphi_2}\hat{a}^\dagger_I + R_2\hat{a}^\dagger_{v_2}\right) \tag{17}$$

$$\hat{a}^\dagger_{p_3} = \gamma_3\left(T_b\hat{a}^\dagger_B + R_b\hat{a}^\dagger_C\right)\hat{a}^\dagger_I \tag{18}$$

Starting from the input state vector (1) and applying the field operator transformations (16)–(18), after some straightforward algebra one gets the output state vector

$$\begin{aligned}|\psi_{\text{out}}\rangle = \frac{1}{\mathcal{N}}\Big(&T_2 e^{i\varphi_2}\left(\gamma_1 R_a T_1 e^{i\phi_1}e^{i\varphi_1} + \gamma_2 T_a e^{i\phi_3}\right)|1_A 1_I\rangle\\ &+\left(\gamma_1 R_a T_1 R_2 e^{i\varphi_1}e^{i\phi_1} + \gamma_2 T_a R_2 e^{i\phi_3}\right)|1_A 1_{v_2}\rangle\\ &+\gamma_1 R_a R_1 e^{i\phi_1}|1_A 1_{v_1}\rangle\\ &+\left(R_b T_2 e^{i\phi_2}e^{i\varphi_2}\left(\gamma_1 T T_1 e^{i\phi_1}e^{i\varphi_1} + \gamma_2 R_a e^{i\phi_3}\right) + \gamma_3 T_b\right)|1_B 1_I\rangle\\ &+R_b R_2 e^{i\phi_2}\left(\gamma_1 T_a T_1 e^{i\phi_1}e^{i\varphi_1} + \gamma_2 R_a e^{i\phi_3}\right)|1_B 1_{v_2}\rangle\\ &+\gamma_1 T_a R_b R_1 e^{i\phi_1}e^{i\phi_2}|1_B 1_{v_1}\rangle\\ &+\left(T_b T_2 e^{i\phi_2}e^{i\varphi_2}\left(\gamma_1 T_a T_1 e^{i\phi_1}e^{i\varphi_1} + \gamma_2 R_a e^{i\phi_3}\right) + \gamma_3 R_b\right)|1_C 1_I\rangle\\ &+T_b R_2 e^{i\phi_2}\left(\gamma_1 T_a T_1 e^{i\phi_1}e^{i\varphi_1} + \gamma_2 R_a e^{i\phi_1}\right)|1_C 1_{v_2}\rangle\\ &+\gamma_1 T_a T_b R_1 e^{i(\phi_1+\phi_2)}|1_C 1_{v_1}\rangle\Big)\end{aligned} \tag{19}$$

where $\mathcal{N}$ is a normalization constant. By imposing $\phi_1 = \phi_2 = \phi_3 = 0$ equation (19) migrates into equation (3) from Section 3.

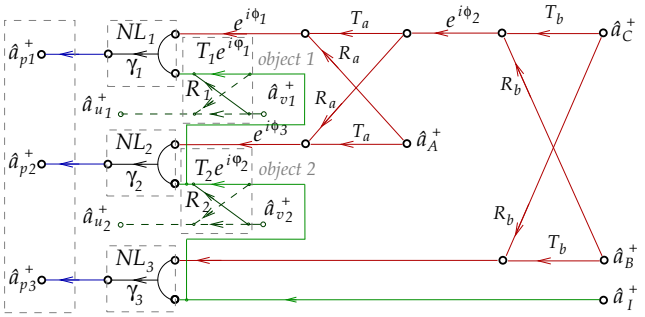

Fig. 4. The proposed Gedankenexperiment described with the graphical method. We are interested in finding the input-output (creation) field operator transformations $\hat{a}_{p_k}^\dagger = f_k\left(\hat{a}_A^\dagger, \hat{a}_B^\dagger, \hat{a}_C^\dagger, \hat{a}_I^\dagger\right)$ i.e. the (operator) functions f_k with $k = 1, 2, 3$.

C Generalization of the previous results

We generalize here the results from Section 4. Using the output wavevector from equation (19) and following the same approach from Section 4, the singles detection probability at detector D_B is found to be

$$P_B \sim \left|R_bT_2e^{i\phi_2}e^{i\varphi_2}\left(\gamma_1T_aT_1e^{i\phi_1}e^{i\varphi_1}+\gamma_2R_ae^{i\phi_3}\right)+\gamma_3T_b\right|^2 + |R_bR_2|^2|\gamma_1T_aT_1e^{i\phi_1}e^{i\varphi_1}+\gamma_2R_ae^{i\phi_3}|^2+\gamma_1^2|T_aR_bR_1|^2 \quad (20)$$

The condition given by equation (9) for making object 2 invisible becomes in this case

$$\gamma_1T_aT_1e^{i\phi_1}e^{i\varphi_1}+\gamma_2R_ae^{i\phi_3}=0 \quad (21)$$

It is obvious now that the delays bring no new elements in our condition: the phase shifts ϕ_1 and ϕ_3 can be grouped together and eventually absorbed into φ_1. Moreover, ϕ_2 is useless in respect with any invisibility condition regarding object 2. If condition (21) is satisfied, the single photocount probability at D_B is

$$P_B \sim \gamma_1^2|T_aR_bR_1|^2+\gamma_3^2|T_b|^2 \quad (22)$$

The coincidence counts at the detectors D_B and D_I can be equally computed yielding $P_{B-I} \sim \gamma_3^2|T_b|^2$. It is not difficult to show that the condition for cancelling the dependence of the coincidence counts at D_A and D_I on T_2 (i.e. $\gamma_1R_aT_1e^{i\phi_1}e^{i\varphi_1}+\gamma_2T_ae^{i\phi_3}=0$) cannot be simultaneously satisfied with equation (21).

References

1. D. C. Burnham, D. L. Weinberg, Phys. Rev. Lett. **25**, 84 (1970)
2. D. N. Klyshko, Sov. Phys. JETP Lett. **6**, 23 (1967)
3. C. K. Hong, L. Mandel, Phys. Rev. A, **31**, 2409 (1985)
4. M. H. Rubin, D. N. Klyshko, Y. H. Shih, A. V. Sergienko, Phys. Rev. A, **50**, 5122 (1994); W. P. Grice, I. A. Walmsley, Phys. Rev. A, **56**, 1627 (1997); T. E. Keller, M. H. Rubin, Phys. Rev. A, **56**, 1534 (1997)
5. P. Kwiat, K. Mattle, H. Weinfurter, A. Zeilinger, A. Sergienko, Y. Shih, Phys. Rev. Lett. **75**, 4337 (1995)
6. C. K. Hong, Z. Y. Ou, L. Mandel, Phys. Rev. Lett., **59**, 2044 (1987)
7. T. Pittman et al., Phys. Rev. Let. **77**, 10 (1996)
8. Z. Y. Ou, X. Y. Zou, L. J. Wang, L. Mandel, Phys. Rev. Lett., **65**, 321 (1990)
9. Z. Y. Ou, L. J. Wang, L. Mandel, Phys. Rev. A, **40**, 1428 (1989)
10. Z. Y. Ou, L. J. Wang, X. Y. Zou, L. Mandel, Phys. Rev. A, **41**, 566 (1990)
11. X. Y. Zou, L. J. Wang, L. Mandel, Phys. Rev. Lett. **67**, 318 (1991)
12. G. B. Lemos *et al.*, Nature, **512**, 409 (2014)
13. A. Heuer, R. Menzel, P. W. Milonni, Phys. Rev. Lett. **114**, 053601 (2015)
14. D. A. Kalashnikov *et al.*, Nature Photonics, **10**, 98 (2016)
15. D. S. Simon *et al.*, Int. J. Quantum Inf., **12**, 1430004 (2014)
16. U. Leonhardt, Rep. Prog. Phys. **66**, 1207 (2003)
17. R. Loudon, *The Quantum Theory of Light*, (Oxford University Press, Third Edition, 2003)
18. S. Ataman, Eur. Phys. J. D **68**, 288 (2014)
19. S. Ataman, Eur. Phys. J. D **69**, 44 (2015)
20. H. M. Wiseman, K. Mølmer, Phys. Lett. A **270**, 245 (2000)
21. T. J. Herzog, J. G. Rarity, H. Weinfurter, A. Zeilinger, Phys. Rev. Lett. **72**, 629 (1994)
22. Ö. Süzer, T.G. Goodson III, Opt. Express. **16**, 20166 (2008)
23. A. Divochiy *et al.*, Nature Photonics **2**, 302 (2008)